Aero-Structural Optimization of Sailplane Wings

Bruno Jorge Pereira Cadete
133802-B

Academia da Força Aérea / Instituto Superior Técnico
Sintra, Portugal

December 2011

Abstract

This article presents a framework for the multi-disciplinary design analysis and optimization of sailplane wings. A literature review on the studies from various authors is presented and used as base for the establishment of the multi-disciplinary optimization (MDO) framework. The approach used employs a multi-disciplinary feasible architecture. The geometric parametrization method employed follows a free-form deformation method. To solve the aero-structural problem, a panel method coupled with a finite-element solver is implemented. The coupled non-linear system is solved using an approximate Newton-Krylov approach. The optimization algorithm uses sequential quadratic programming, where the gradients are evaluated using the adjoint method. A real sailplane wing, based on the L-23 Super Blanik from the Portuguese Air Force, is used as test case. Single disciplinary analysis assess the capabilities of the disciplinary modules of the framework. Results are presented for a drag minimization problem using aerodynamic and multi-disciplinary optimizations. They reveal important trade-offs between disciplinary optimum and multi-disciplinary optimum at the preliminary design stage.
Keywords: Aero-structural problem, Multi-disciplinary optimization, Free-form deformation method, Panel method, Finite-element method, Sailplane wings.

1. Introduction

In aircraft preliminary design, it is very important to take into account not only the elegance of the aircraft but also its disciplinary constraints. Typically, the integration of the disciplines is only handled in the latter stages of the design, through prototype testing. However, with the emergence of a new generation of aircrafts, with unusual design approaches like the blended-wing body, should a "build and test" approach be used, it would be too time and resources consuming, as no past experience exist. This is where the power of multi-disciplinary optimization (MDO) techniques can make a difference.

However, the utilization of MDO in aircraft design has only fully emerged as a technique viable for aircraft design in the last two decades. With MDO approach, time can be gained and a better and unusual feasible result may be achieved, without the normal approach of "do as others have done" or "build and then test".

2. Gliding and Soaring

2.1. Brief History

The first spoken tentatives, of men trying to lift themselves into the air are dated in 200 BC in China, with hot air balloons and kites. Later, in Europe, some early attempts of gliding were made, like the Eilmer of Malmesbury that flew 200 meters before crashing. In the 18^{th} century, a first rigorous study of flight physics was made by Sir George Cayley. While trying to improve a glider, he invented most of basic aerodynamics principles, such as "lift" and "drag". In the 1820's gliders were of great relevance to the powered aviation as they were the predecessors to the Wright Flyer I. Though, losing relevance in the early 1990's to hot air balloons and powered aircrafts, after 1919, sailplanes would emerge again, as the Treaty of Versailles imposed restrictions on powered aircraft usage in Germany and enforced German engineers to develop ever more efficient gliders and gliding techniques. During the following years, gliding sport spread to other countries around the world. Since 1970's, the evolution of gliders has been following the exponential evolution of structural engineering, material science, computational fluid dynamics and electronics.

2.2. Principles of Gliding and Soaring Flight

The principles of flight for sailplanes are the same as for all the aircrafts: it is the action of forces on the entire vehicle that allows it to stay airborne. As the wing airfoil exerts a force on the air to change its direction, the air exerts a force on the wing, equal in size but opposite in direction. The resultant force manifests as differing pressures p and flow velocities at the two sides of the wing surface. This force is

obtained by integrating p and the wall stress τ over the wing surface (Anderson, 2001). Lift L an drag D, are the forces components in the normal and stream-wise flow directions, respectively. In aerodynamics, the dimensionless force coefficients, lift and drag coefficients, are defined as

$$C_L \equiv \frac{L}{q_\infty S} \qquad \text{and} \qquad C_D \equiv \frac{D}{q_\infty S}, \quad (1)$$

where the free-stream dynamic pressure is defined as q, being $_\infty$ the free-stream condition. Another quantity of interest in aerodynamics is the pressure coefficient, defined as

$$C_p \equiv \frac{p - p_\infty}{q_\infty}. \quad (2)$$

2.3. Sailplane Performance

Performance can be measured by the maximum range or endurance. Assuming that the sailplane is at equilibrium, the equations of motion are

$$\begin{aligned} D - W sin(\gamma) = m\dot{V} = 0, \\ L - W cos(\gamma) = m V_S = 0, \end{aligned} \quad (3)$$

where γ is the flight path angle and $V_S = V sin(\gamma)$ is the sinking speed. Dividing one equation by the other, the relation between the flight path angle and the L/D ratio arises, $tan(\gamma) = -D/L = -1/(L/D)$. This expression gives a negative flight path angle as would be expected in gliding. Thus, defining glide angle as the negative of the flight path angle, the expression turns to $tan(\gamma_1) = 1/(L/D)$, where the γ_1 is the glide angle. Therefore, this angle is independent of the weight and its lowest value corresponds to the higher L/D ratio.

The gliding range, R, corresponds to the longest distance traveled along the ground during the glide descent. Assuming an initial altitude, h_1 and a ground altitude, h_2, it can be calculated from

$$R = \frac{h_1 - h_2}{\tan \gamma_1} = \frac{L}{D}(h_1 - h_2). \quad (4)$$

Here the ratio L/D is also called *"gliding ratio"*.

Gliding endurance consists of achieving the longest duration of flight. For that to be possible, the gliding angle has to be kept at a minimum, thus, generating a minimum sinking speed. Mathematically, this speed is given as

$$V_S = V sin(\gamma) = -V\frac{D}{W} \approx -\sqrt{\frac{W}{1/2\rho S}\frac{C_D}{C_L^{3/2}}}. \quad (5)$$

As the gliding angle is usually small, a small angle assumption ($L = W cos(\gamma) \approx W$) can be made. To minimize the sinking rate, the quantity $C_D/C_L^{3/2}$ and the weight must be minimized.

3. Multi-Disciplinary Analysis and Optimization

3.1. MDO History in Aeronautic Industry

An aircraft can be described as a complex multi-disciplinary system. The design of an aircraft generally consists of a hierarchical sequence of steps starting from conceptual design phase through a preliminary design phase and a detailed design phase ending in prototype building and testing. Since the beginning of the aeronautical industry, the design was performed by various individual teams, each with expertise in a specific discipline. These teams were involved in the aircraft design and did not work independently of each other. Instead, they used its members experience to develop a workable design, usually sequentially from an outline of the shape of the body, which then, would be modified by other disciplinary teams. This methodology was widely used and led to good results in the early times of the aeronautical industry. However, in the 80's there were two major developments that led to the modification of the methodology used by aircraft design engineers, the emerging of computer-aided design (CAD) and the change in the acquisition policy from from a performance-centered approach, to one that emphasis life-cycle cost issues. These major developments led to the emergence of multi-disciplinary design teams and MDO. Performing computational analysis, together with numerical optimization, made MDO emerge as one of the fields of engineering that can provide optimal solutions to aircraft design problems. Tools such as CFD and computational structural mechanics (CSM), that can perform fast high-fidelity numerical analysis are coupled together in MDO to produce an optimal solution between multiple disciplines. Many studies addressed the best way to implement MDO and shown that a modular scheme is the best way to accommodate the individual disciplines in an MDO framework (Isaacs et al., 2003). Today, the majority of the MDO studies focuses on two of the main disciplines of aircraft design, aerodynamics and structures, which together, form the so called aero-structural optimization problem. Ultimately, there are two factors that have slowed industry's adoption of MDO (Kenway et al., 2010). The first is the increased computational cost and complexity of the optimization problems when running high-detail analysis. The second, and perhaps the main factor, is that the inter-disciplinary nature of MDO strategies does not integrate easily into well established (single) disciplinary design groups. Yet, there are proven cases where MDO has performed successfully in the conceptual and preliminary design stages of aircraft design (Liebeck, 2004).

3.2. MDO Problem Definition

An MDO problem can be seen as a system containing multiple sub-systems. Each of these subsystems handles a discipline, having implicitly a set of discipline governing equations. These, solved with an appropriate set of inputs, will generate a disciplinary state. A generalized representation for these equations is

$$y_i = f(x_i, y_i, z), \quad i, j = 1, ..., n, \quad j \neq i, \tag{6}$$

where n is the number of disciplines, denoted by i, representing the i^{th} discipline, x_i is the local variable vector, the vector y_j corresponds to interdisciplinary couplings, and z denotes the global variable vector.

When provided with an set of design variable inputs, the sub-systems will generate discipline feasible states and outputs. The set of inputs consist not only of disciplinary variables but also of coupling variables. The last provide information regarding the state of the other disciplines. In its formulation, the problem can be compared to an simple optimization problem as three entities need to be defined: the objective function, the design variable set and the constraint set.

The MDO problem has two main differences compared to a optimization problem with a single discipline (Yi et al., 2007): the fact that each discipline needs inputs that result from other disciplines and that there are common objective functions, design variables and constraints, shared by the disciplines. These differences make MDO problems larger and more complex than disciplinary problems.

In MDO problems, both the design variable and constraint sets can be grouped, based on their effect in multiple disciplines, in local or global variables. Likewise, there are local and global constraints. There are also two types of optimization constraints. They can set a range of values for the variables (inequality constraints) or they can be residual equations solved only at optima (equality constraints). Ultimately, the way how an MDO problem is converted into one or more standard optimization problems is what defines the MDO strategy or architecture.

3.3. MDO Architectures

A wide variety of MDO architectures have been proposed and evaluated either by defining a different problem formulation or by finding the most efficient optimization algorithms (MDO Technical Commite, 1991). Also, research in the advantages and disadvantages of each MDO architecture has been made by many authors, such as Perez et al. (2004). An important aspect of approaching an MDO problem is the fact that its formulation can vary according to the architecture used. Before the architecture choice, there are some aspects that have to be examined, like for instance, the number of the disciplines involved, the number and type of design variables. Other aspect is the method used to solve the optimization problem created. Currently must studies use gradient-based methods (Alexandrov and Hussaini, 1997). The MDO architectures can be classified in: single-level methods and multi-level methods. Single-level methods, like Individual Discipline Feasible (IDF) or Multi-Disciplinary Feasible design (MDF), include only one optimizer at a system-level, which runs a system analysis in each step and has authority over the global system (Dennis and Lewis, 1994). Multi-level methods which include Concurrent Subspace Optimization (CSSO) (Sobieszczanski-Sobieski, 1988) and Bi-level Integrated Systems Synthesis (BLISS) (Sobieszczanski-Sobieski et al., 1998), create for each discipline a subspace, in which optimizations are made. Each individual discipline has a separate local optimizer that modifies the design. Also, there is a global optimizer at the system-level, that manages the relationship between disciplines. These methods create a hierarchical structure in the global system, where each disciplinary sub-group was some degree of freedom to work independently.

Extensive study of architectures comparison was not the objective of this thesis. Thus, only a brief description of some of advantages or disadvantages of the most common architectures will be made to enframe the decision made, for the MDO architecture to use in the established MDO framework. A comparison study made by Perez et al. (2004), evaluated MDO architectures using an extended set of proposed metrics which took into consideration optimization and formulation characteristics. Its results show MDF as the most accurate method since it performs full disciplinary system analysis. Unfortunately, its efficiency suffers with the increase in complexity, so its better used with simple system analysis (Yi et al., 2007). Martins and Tedford (2006) showed conclusions, consistent with the mentioned above, as in terms of robustness, MDF proved to be able to consistently return optimal solutions, with the least number of failures.

As such, MDF architecture was chosen in the present work.

3.4. Multi-Disciplinary Feasible

The MDF architecture is often viewed as the most traditional approach. In it, an optimizer is placed over an MDA module. This takes in the optimizers set of design variables, optimal global z and local variables x and iterates over the disciplinary analyses until a consistent set of coupling variables has been generated. Then, the complete variable set is used to compute the values of the objective and constraint functions. The MDA is typically solved

by a block-iterative procedure like the Gauss-Seidel iteration and is considered to be converged once the coupling variables have remained constant within a specified tolerance over successive iterations. The fact that it requires a solution of the MDA at each design point, ensures that a multi-disciplinary feasible solution is present throughout the optimization process, so if prematurely, a physically realizable design point will still be achieved. The computation of the MDA at each design point also negates the need to include the discipline coupling variables as optimization variables. A schematic representation of the flow of information using MDF architecture is presented in Fig. 1. Mathematically, this architecture can be described as

$$\begin{aligned} \underset{z,x}{\text{Minimize}}: \quad & f(z, y_i(x, y_j, z), x), \\ \text{where} \quad & i, j = 1, ..., n \qquad j \neq i \\ \text{s.t.:} \quad & g(z, y_i(x, y_j, z)) \leq 0, \end{aligned} \tag{7}$$

where f is the objective function and g represent all the global and local system constraints. The sensitivity analysis method employed is important as the use of gradient-based optimizers can result in low performance. If either a finite difference or complex-step method is used to compute the the sensitivities of the objective and constraints with respect to the design variables, an MDA must be solved for each sensitivity which can have a prohibitive cost.

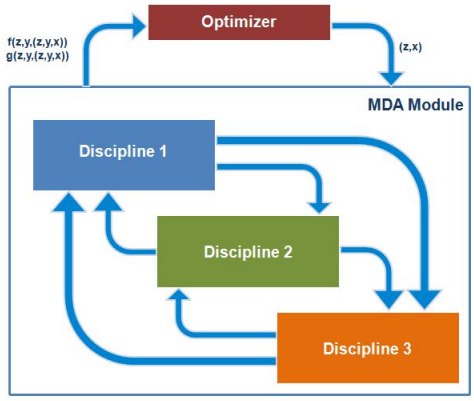

Figure 1: Multi-disciplinary design feasible architecture.

4. MDO Framework

The first step to define in the MDO framework was a proper geometric parametrization method. Kenway et al. (2010) presented a method that follows a CAD-free geometry parametrization approach. As this method presented good results and the fact that having no need to use a CAD software for the geometric parametrization is an advantage itself, it was chosen to be used within the MDO framework.

Using tools developed at the University of Toronto (UoT) MDO Lab, two aerodynamic disciplinary solvers and one structural solver were tested. Thus, based on the fidelity of the results, the ease of implementation and coupling, two were chosen: a panel code named *Tripan* for the aerodynamics, and a parallel finite-element analysis package named *TACS* for the structures. As result of the choice of an MDF architecture only one global optimizer was needed. After testing some optimizers, the one chosen was *SNOPT* (Gill, 2008), a sparse sequential quadratic programming (SQP) algorithm. *SNOPT* is fully integrated in the *pyOpt* MDO Lab module (Perez et al., 2011). Thus, this object-oriented framework for formulating and solving non-linear constrained optimization problems was used to handle the optimization process.

4.1. MDO Tool Structure

With the framework defined a modular structure was established for the MDO tool. Also an interface had to be elected. Following the work of the authors previously mentioned, the interface chosen for the tool was through script files. Although the core components were mostly written in Fortran and C languages, all were already wrapped in Python language. This fact made clear the choice to go with Python as the scripting language. With the interface, disciplinary solvers and optimizer components chosen, the structure to the final MDO tool was created. Figure 2 shows the scheme of the overall MDO tool structure established and used to run the aero-structural optimization of sailplane wings.

4.2. Geometry Module

In aerodynamic analysis, a model of the *"wetted surface"* or *"outer mold line"* (OML) of the wing is required. On the other hand, structural analysis of that same wing, require not only the OML but also a description of the internal aircraft structure components like ribs, skins, spars and stiffeners. To implement the CAD-free approach method that uses both spline and free volume deformation (FFD) based approaches, a set of geometry tools from the MDO Lab was used. The FFD volume base approach was first presented by Sederberg and Parry (1986). A good physical analogy that is often used to explain the FFD approach, is the one where an object (or objects) that one wants to deform, is embedded in a clear, flexible, plastic material. The object is assumed to be flexible, so that it deforms along (in a consistent motion) with the material surrounding it. The use of this technique allows easier parameterizations of solid object models since it is not the object geometry itself that is parametrized but the volume where it is embedded. As a consequence, this technique only uses a set of design variables which will produce the desired modifications to the object, rather than the objects geometry itself.

The tools used to implement the FFD approach

include functionalities with both B-spline curves and surfaces and are called *pySpline* and *pyGeo*. *pySpline* is a underlying B-spline library for curves and surfaces developed by Gaetan Kenway for the MDO Lab of the UoT.

For configurations of some complex geometry, as an airplane wing, using only isolated curves, surfaces or volumes are not enough. It is necessary to combine the entities together in some topological manner. *pyGeo* is the tool that handles this function, working as a geometry surfacing engine. It performs multiple functions including producing surfaces from cross sections, fitting surfaces and has built-in design variable handling.

Finally, the tool used to generate the finite-element analogues to the structural members within the wing is called *pyLayout*. This Python module is used for automatic parametric structure generation of wings. Given a description of the structural layout within the OML of the wing, *pyLayout* automatically generates a wing-box finite-element model that mimics the structural characteristics of the real wing.

4.3. Aerodynamics Module

Modern gliders have average speeds to fly is in the range of 20m/s to 30m/s, which for an average flight altitude of 1000 meters, give low Mach numbers. This is an important fact, as it allows the airflow to be considered incompressible. Also, modern sailplanes are designed to be smooth and have wing geometries that avoid flow separation and minimize viscous effects. Therefore, is a valid assumption to consider an inviscid, incompressible and irotational model to accurately simulate flow in which a sailplane flies. Reminding Sub-section 4, two flow solver were tested: the *SUmb* and the *Tripan*. *SUmb* is a multi-block structured flow solver developed in the Stanford University Center for Integrated Turbulence Simulations (CITS). It is a code that solves the compressible Euler, laminar Navier-Stokes and Reynolds-Averaged Navier-Stokes equations (Weide et al., 2005). On the other hand, *Tripan* is an unstructured, three-dimensional panel code. The two modules could be used for the aerodynamic analysis, however, as the course of the work revealed, the *Tripan* flow solver was better suited to be coupled with the structural solver. Though not implemented, *SUmb*, as an high-fidelity model, was validated and used to verify the accuracy of *Tripan*. *Tripan* uses a first-order panel method with constant source and doublet singularity elements, distributed over the surface of a body, discretized with quadrilateral and triangular panels (Anderson, 2001). This method allows the calculation of aerodynamic forces, moments and pressures for inviscid, incompressible, external lifting flows. Yet, it has well known limitations, especially of accuracy when computing drag (Smith, 1996).

To perform the aerodynamic analysis *Tripan* determines the source strengths based on the onset flow conditions while the boundary conditions for the doublet strengths constitute a dense linear system, represented by

$$\mathbf{A}(u, w) = 0, \tag{8}$$

where u and w are the vectors of the structural and aerodynamic state variables. The linear system represented in Eq. 8 is solved using the parallel, linear algebra routines in PETSc (Balay et al., 2004) and using the Krylov subspace method generalized minimal residual method (GMRES) (Saad and H.Schultz, 1986) with a block Jacobi Incomplete LU(ILU) preconditioner formed using a sparse approximate-Jacobian.

4.4. Structures Module

Structures represent the second discipline in the proposed MDO. The methods and tools chosen to perform the structural analysis followed the most recent studies published by Kennedy and Martins (2010) and Kenway et al. (2010). Thus, the tool used for the structural analysis was a finite-element code developed by Graeme J. Kennedy of UoT called Toolkit for the Analysis of Composite Structures (*TACS*). This code was created for the

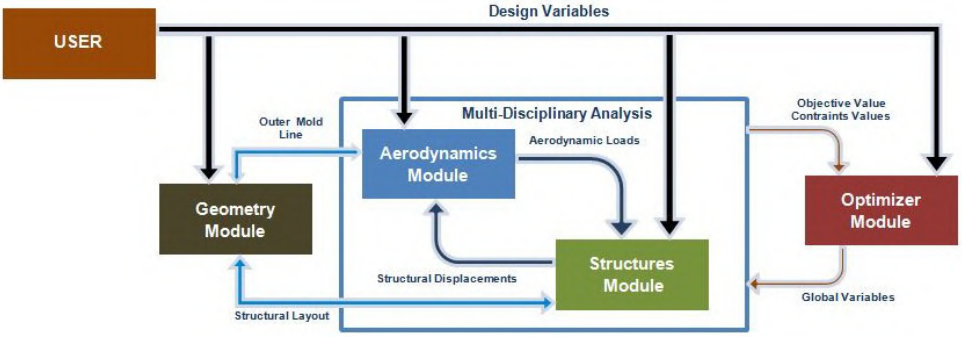

Figure 2: MDO tool structure established for the aero-structural optimization of sailplane wings.

analysis of stiffened, thin-walled, composite structures using either linear or geometrically non-linear strain relationships. It can use higher-order finite-elements to enhance the stress prediction capability. The residuals of the structural governing equations are expressed as

$$\mathbf{S}(u, w) = \mathbf{S}_c(u) - \mathbf{F}(u, w), \tag{9}$$

where where u is a vector of displacements and rotations (structural state variables), w is a vector of aerodynamic state variables, S_c are the residuals due to conservative forces and internal strain energy and F are the follower forces due to aerodynamic loads.

The Jacobian of the structural residuals involves two terms. The first is the tangent stiffness matrix $\mathbf{K} = \partial \mathbf{S}_c / \partial u$. The second is the derivative of the consistent force vector with respect to the structural displacements. These terms are computed using a matrix-free approach. Mathematically the Jacobian of the structural residuals is represented by the expression in Equation 10.

$$\frac{\partial \mathbf{S}}{\partial u} = \mathbf{K} - \frac{\partial \mathbf{F}}{\partial u}. \tag{10}$$

TACS uses the Krylov subspace method GMRES and the the Krylov method GCROT (Hicken and Zingg, 2010), to solve the non-symmetric, linear systems of Eq. 10. It handles stress constraints by applying a local failure constraint at each Gauss point in the finite-element model. These local failure constraints compute a load factor, λ_k, required for that point to fail. The load factor implies that the current point will fail at λ_k times the current stress level. For a safe-life design, the criterion $min\{t_k\} > Fs$ is applied, where Fs is the safety factor. This method applied to an optimization has some specificities. Instead of using the minimum value directly, a Kreisselmeier-Steinhauser (KS) constraint aggregation technique is applied to groups of these local constraints (Wrenn, 1989). Normally these groups are aggregated amongst similar structural components. In *TACS*, the KS function is computed as

$$\lambda_{KS} = min\{\lambda_k\} - \frac{1}{\sigma} ln\left[\sum_{i=1}^{N} exp\{-\sigma(\lambda_i - min\{\lambda_k\})\}\right], \tag{11}$$

where σ is a weighting parameter that controls the degree of approximation and λ_{KS} is the aggregated KS value. This approach has the advantage that it reduces the number of constraints required in the optimization, while keeping a conservative approximation, in that λ_{KS} is a lower bound.

4.5. Aero-Structural Coupling

When using a coupling method in an MDO framework, it is important that the level of fidelity in the coupling guarantees the accuracy of the individual disciplines (Martins, 2002). Also, the discretization in each discipline must preserve the geometric consistency during the analysis process.

4.6. Load and Displacement Transfer

The objective of the load-displacement transfer process is to accurately translate the nodal displacements of the structural model to aerodynamic mesh point displacements. In the tool established for this thesis, the load and displacements transfer scheme follows the method described by Brown (1997). This method rely on extrapolation functions for the displacements of the internal structure to obtain the aerodynamic mesh displacements. These extrapolation functions must satisfy two conditions. The first one is that these functions must accurately reproduce a rigid body motion. The second condition is that the resulting aerodynamic mesh displacement field must be continuous over the whole surface. To extrapolate the structural displacement field, each point of the aerodynamic mesh, $\mathbf{x}_A$, must be associated to a point on the structural model, $\mathbf{x}_S$. The association is made so that the distance between the two points is minimized. When the association is made, it remains the same either in the initial and perturbed geometries. The link between the point in the aerodynamic mesh and the point on the structural model is made through the vector, $\mathbf{r} = \mathbf{x}_A - \mathbf{x}_S$, which maintains its position and orientation relative to the associated finite-element point. The displacement of the aerodynamic mesh point, $\mathbf{u}_A$, can then written as

$$\mathbf{u}_A = \mathbf{u}_S - \mathbf{r} \times \theta_{\mathbf{S}}, \tag{12}$$

where u_S is the displacement of the structural model point, and θ_A and θ_S are equal rotations ($\theta_A = \theta_S$). The load transfer procedure is similar to the displacement transfer. The pressures calculated by the aerodynamic flow solver are transferred to the structural nodes through aerodynamic mesh points. To perform the transfer, an appropriate cell and the parametric location of each mesh point within this cell, is identified. The aerodynamic pressures are then calculated by using bilinear interpolation on the surface of the aerodynamic mesh. The distributed pressure load, applied to a structural finite-element model, must first be transformed into an equivalent set of nodal forces. This transformation has two requirements. The first is that the resultant nodal forces and moments are the same as those that result from the pressure field for each element. The second is that the load transfer must be conservative. To ensure the former, the virtual work performed by the load vector, $\mathbf{f}$, undergoing a virtual displacement of the structural model, δu, must be equal to the work performed

by the distributed pressure field, p, undergoing the equivalent displacement of the aerodynamic mesh, u_A,

$$\delta W_S = \delta W_A. \tag{13}$$

4.7. Aero-Structural Solution

The coupled non-linear system of equations is a combination of the aerodynamic and structural residuals, Eqs. 8 and 9, respectively, represented by

$$\mathbf{R}(q, x) = \begin{vmatrix} \mathbf{A}(w, u, x) \\ \mathbf{S}(w, u, x) \end{vmatrix} = 0, \tag{14}$$

where, x are the design variables and q is the combination of aerodynamic and structural states, $q^T = \begin{bmatrix} w^T u^T \end{bmatrix}$. During the solution procedure, a point is considered converged when the relative tolerance of both residuals is reduced below a specified tolerance. However, the stop criterion is applied to each discipline separately, rather than to the aero-structural system, to avoid situations where the initial residual of one discipline is significantly greater than the initial residual of the other.

To solve the aero-structural system in Eq. 14, an approximate Newton-Krylov Method is used. This method results in the linear system of equations for the update, $\Delta q^{(n)}$, expressed as

$$\frac{\partial \mathbf{R}}{\partial q} \Delta q^{(n)} = -\mathbf{R}(q^{(n)}). \tag{15}$$

This method can converge quadratically if the starting point is sufficiently close to the solution and the Jacobian remains non-singular.

However, to achieve convergence when the starting points are far from the solution, the Newton method may have to be globalized with some strategy, to ensure progress is made towards the solution until a suitable starting point is found. So, solving Eq. 15 inexactly for each update is typically more efficient than finding an accurate solution. This is the methodology used, so a tolerance of $\epsilon_{nk} = 10^{-3}$ was set to the Newton update.

4.8. Optimizer

To efficiently achieve a feasible design point, numerical simulations must be combined with automatic optimization procedures. These are optimization algorithms created to find the design variables that yield the optimum point for a design problem.

At the moment, there are two main categories of algorithms. The first includes the *'zeroth order methods'*, such as grid searching, random searches and evolutionary algorithms (Alexandrov and Hussaini, 1997). The second category includes the *'gradient-based methods'*. These methods use the value of the objective function and the value of its gradient with respect to the design variables. These methods have the advantage that they will converge to the optimum with a smaller number of function evaluations. In optimizations like those in aircraft MDO, that feature a large number of design variables, expensive high-fidelity analyses and a smooth design space, the benefit goes for the gradient-based methods. Therefore, a gradient-based strategy is also employed in the established MDO tool.

The optimization algorithm used is called *SNOPT* (Gill, 2008). This module has been compiled with a Python interface, named *pySNOPT*, for an easy integration in MDO frameworks.

Efficient gradient-based optimization requires the accurate and efficient computation of the objective and constraint gradients. Following Martins (2002), an aero-structural adjoint method that is based entirely on analytical derivatives was used. The implicit aero-structural adjoint equations are

$$\frac{\partial \mathbf{R}^T}{\partial q} \psi = \frac{\partial \mathbf{f}}{\partial q}, \tag{16}$$

where ψ refers to the adjoint vector and f is either an aerodynamic or structural function of interest. The total derivative is then determined using

$$\frac{d\mathbf{f}}{dx} = \frac{\partial \mathbf{f}}{\partial x} - \psi^T \frac{\partial \mathbf{R}}{\partial x}. \tag{17}$$

Once the adjoint vector ψ has been determined, the total sensitivities must be computed using Eq. 17.

5. Results

5.1. Case Study

The case study chosen to run the proposed MDO is the L-23 Super Blanik sailplane wing. The LET L-23 Super Blanik sailplane wing is an all-metal, cantilever, mono-spar, tapered wing that consists of two assemblies. Its main geometry parameters of the wing are summarized in the Table 1. The

Table 1: Geometry parameters for the case study.

Parameter	L-23	
Span	16.2	m
Reference Area	19.15	m^2
Taper Ratio	0.429	
Dihedral Angle	3	$^\circ$
Sweep Angle	-5	$^\circ$
Twist Angle	-3	$^\circ$

real structural layout of the L-23 wing was used as reference for its structural modeling. Therefore, the wing internal layout is modeled with seventeen ribs, one main spar and an auxiliary spar. The thickness values for the structural components were set to 5 mm in the skin, 10 mm in the spars and 8 mm in the ribs. Although it is not the exact modeling of the real layout, it was the best approximation that was possible to recreate using the geometry module. Also, a maximum take-off weight of

530kg was used (L-23 sailplane maintenance manual, 2011). Figure 3 shows the geometry objects created for the L-23 case study. As observable, the aerodynamic meshes are almost perfectly coincident with the OML of the desired wing geometry. Also, the structural models of the wing box fits perfectly in the OML. So, the use of *pySpline* in combination with *pyGeo* has proven to provide quality aerodynamic geometry objects and the use of *pyLayout* also assured well suited internal structural layouts.

Figure 3: Geometry objects for the L-23 case study.

5.2. Aerodynamics

5.2.1 Verification of *Tripan*

To verify the fidelity of the aerodynamics simulation code, a verification of *Tripan* with another code that could be validated, using experimental data available, was the methodology used. Thus, the first task was to validate *SUmb* so that it could be used for the *Tripan* verification. To fulfill this, a classical study of three dimensional turbulent transonic flows was chosen, the rebuilding of the ONERA M6 wing wind tunnel experiments (Schmitt and Charpin, 1979). In this, the flow over the ONERA M6 wing was studied by testing it in a wind tunnel at transonic Mach numbers and various angles-of-attack. The Reynolds numbers were about 12 million based on the mean aerodynamic chord. Records were taken of the upper and lower pressures for seven wing sections along the span. To rebuild the wind tunnel tests, the flow was numerically build using *SUmb*. The flow conditions for the simulation were set to match the experiment values of Mach number, Reynolds number and angle-of-attack. The ONERA M6 wing is a swept, semi-span wing with no twist. It uses a symmetric airfoil. The semi-section of the airfoil is the ONERA D section (Schmitt and Charpin, 1979). To improve this study, a cross comparison of the obtained results was done against the *WIND* code results from NASA (Slater, 2008).

A sample of the comparison between the sectional Cp obtained with *SUmb* with the experimental data and with *WIND* is presented in Fig. 5. The accuracy of the Cp measurements for the experimental data was determined to be +/- 0.02. From the results, it is clear that the two numerical solvers are

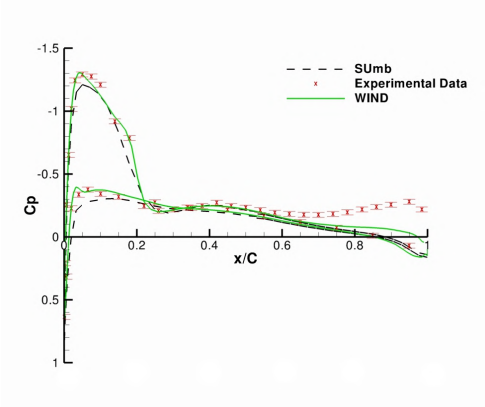

Figure 4: Sample *SUmb* validation results.

very close to one another. Overall, its clear that the agreement between numerical solvers is good. Compared to the experimental data, the flow structure computed by the two numerical solvers seems to be not sharp enough in the shock resolution. However, for the validation purpose it is meant for, i.e., to validate an incompressible, inviscid flow solver (*Tripan*), the good agreement between *SUmb*, *WIND* and experimental data was considered enough.

The next step was the verification of *Tripan* using *SUmb*. To this purpose an incompressible, inviscid external flow was used. The wing geometry used to perform the comparison analysis was the ONERA M6 wing. A sample of the results for the *Tripan* validation is shown in Fig. 5 presenting Cp distribution for one section at 85% of the wing span. Results show that the two numerical flow solvers are very close to one another. Only in the trailing-edge, a slightly difference is noted. In sum, the good agreement between solvers verify that *Tripan* provides accurate results when simulating incompressible inviscid flows.

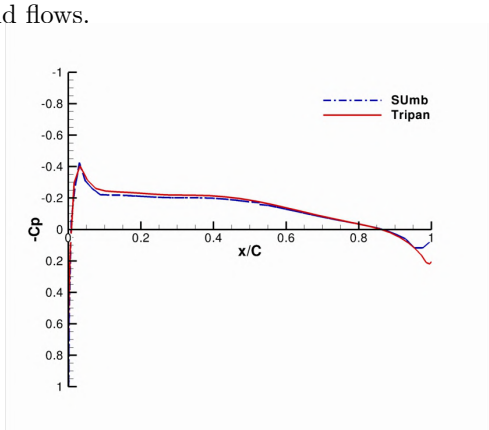

Figure 5: Sample *Tripan* verification results.

5.2.2 Aerodynamic Analysis

Once verified the code used in the aerodynamics module, aerodynamic analysis on the case study

was run. As an academic exercise, there are no imposing requirements for the simulations performed. However, as the case study is a sailplane wing, the conditions chosen were those from a cross-country soaring flight at 1000 m, with a velocity of $25m/s$. Table 2 summarizes the free-stream conditions defined in the simulation, based on the 1976 standard atmosphere up to 230,000 ft. Before running the

Table 2: Flow conditions for aerodynamic analysis.

Design Parameter		
Mach	0.074	
Angle of Attack	3	$^\circ$
Density	1.112	Kg/m^3
Speed of Sound	336.434	m/s

aerodynamic analysis, a convergence study was performed to determine the proper number of panels for the aerodynamic mesh discretization. A range of *Tripan* objects was created from a simple mesh with 150 panels, to a highly refined mesh with 12,150 panels. Then, an aerodynamic analysis was performed on each one of these meshes. To assess the results obtained, a relative error evaluation was performed. In this study, the real value of the aerodynamic quantities is not known, so the value computed for the most refined mesh is used as the best approximation to the real value. Thus, from the various aerodynamic analysis performed, a graphic with the convergence of the results was compiled and presented in Fig. 6. As *Tripan* uses a panel

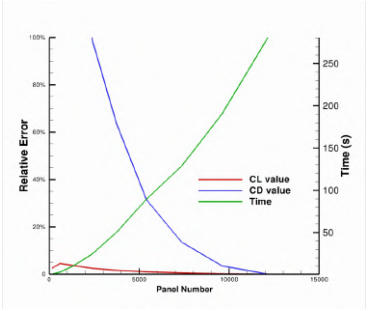

Figure 6: Convergence study on *Tripan* mesh.

code, the error for the lift coefficient converges much faster that the drag coefficient. Although the computed drag value is not accurate, as the code can not compute the total drag, it was important to assess its convergence. Also, the time required to perform the aerodynamic analysis was measured. It is observable that time grows exponentially with the number of panels used. From the results seen, a panel number near 7,000, was considered to give the best relation between accuracy error (approximately 10%) and time to perform the analysis (approximately two minutes).

With every parameter defined, the aerodynamics module of the MDO tool was used to perform the aerodynamic analysis on the case study. Figure 7 summarize the results obtained, which consist of Cp distribution over the wing, Cp over four sections along the wing semi-span and lift distribution over the wing are presented. From the observation of the normalized lift distribution over the semi-span of the wing, one can see that the L-23 wing shows a near constant slope until 75% of the span which then, rapidly increases towards the tip. These results are interesting as they show that the lift distribution is not close to the aerodynamic elliptical optimum. Yet, if one accounts for the fact that, although tapered, the L-23 wing also has a constant twist and sweep angles, then the results seem more comprehensive. Also, this is a real wing, which was already optimized by the manufacturer, taking into account more than aerodynamics, these results are justified. The L-23 more inboard lift results in a weaker bending moment at the wing root. This fact allowed the use of lighter, less strong structural components which consequently reduced the total weight of the wing structure. This is a clear evidence that structures were taken into account when the wing was designed by the manufactured. As for the Cp distributions over wing sections, the L-23 wing sections show high gradients through the major portion of the sections. The increase and decrease of pressure on the upper and lower surfaces are also smooth. These were expected since the L-23 wing airfoil morphs from a NACA 63_{2A}-615 at root to NACA 63_{2A}-612 at tip (both laminar airfoils). These smooth increments and decrements in the Cp are result of the thickness of those airfoils and the fact that they have small sloped surface geometries. It is clear that the airfoils in the L-23 wing have been chosen to provide good results in low speed gliding performance.

A note about the simulation process, near the leading-edge of some sections, as there are some observable deviations that, though subtle, can denounce some numerical errors. This will be remarked for future works.

In summary, the aerodynamic module provided good results performing aerodynamic analysis over the case study, denoting the characteristics of the L-23 sailplane wing.

5.2.3 Aerodynamic Optimization

One of the main objectives in sailplane performance is the maximization of the L/D ratio, to maximize the range of the flight. The next step in the exercises run with the established MDO tool was an aerodynamic optimization of the case study. The initial flight condition for the optimization is the same as that of the aerodynamic analysis, presented in Table 2. The objective function was the L/D ratio. As an academic exercise, there were no im-

Table 3: Aerodynamic optimization parameters for the L-23 wing.

Parameter	Initial Value	Optimized Value	Lower Bound	Upper Bound	
C_L	0.981	0.779	0.779	0.779	
Angle of Attack	3	3.15	-4	7	°
Twist (z/b=30%)	0	0	-10	10	°
Twist (z/b=60%)	0	5	-10	10	°
Twist (z/b=90%)	0	5	-10	10	°
Twist Tip	0	-5	-10	10	°
Chord Scale (z/b=30%)	1	1	0.5	2	
Chord Scale (z/b=60%)	1	0.5	0.5	2	
Chord Scale (z/b=90%)	1	0.5	0.5	2	
Chord Tip	1	0.5	0.5	2	
C_D	0.0143	0.00997			

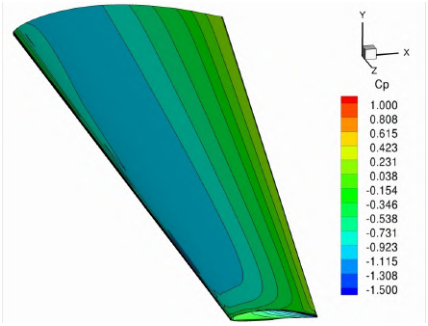

(a) Results for Cp distribution over the wing.

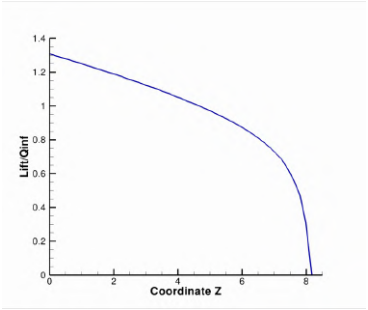

(b) Results for lift distribution over the wing.

Figure 7: Aerodynamic analysis results.

the initial value. So, changes in section chord will reflect in the wing area and, therefore, the aspect ratio and C_L value. A summary of the initial and final parameters of the aerodynamic optimization for the case study is shown in Table 3.

The results verify that, although the initial C_L was different from the requested value, the constraint was fulfilled in the optimization process. In the case study the initial C_L value was higher than the requested so the angle of attack did not have to be increased which allowed the optimizer to start from the beginning making changes in the variable to lower the drag. This is visible in the C_D evolution illustrated in Fig. 8. The values of twist and

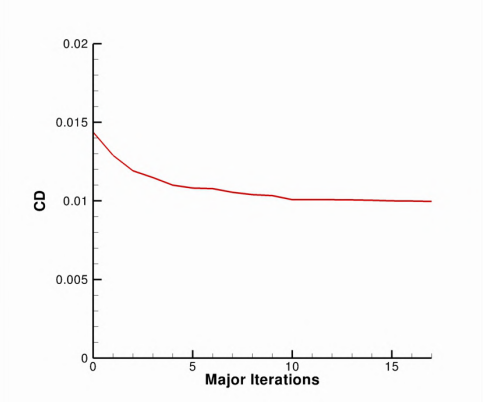

Figure 8: Convergence history for the aerodynamic optimization of the L-23 case study.

posing constraints but those created specifically for this exercise. So, in the case study, a lift constraint was applied. That constraint was set through C_L to equilibrate the weight of the sailplane. With the lift constrained, the range optimization problem is turned into a drag minimization problem. So, using the initial conditions as stated and imposing a minimum lift as constrain, the optimizer had to adjust the geometry variables so that the required C_L is achieved with the minimum drag possible. The geometric design variables chosen are four twist angles and four chord scale factors. The span is fixed to

scale changed as well. The twist group of variables show that once reached a sufficient angle of attack, the optimizer chose to increase the twist angle of the middle sections. Although the final twist values have to be adjusted, since the real wing has a -3° twist, its clear that the optimizer changed the twist angles so a lift distribution closest to the aerodynamic optimal could be reached, therefore, reducing the drag. As for the scale group of variables, it shows a decrease as the sections approach

the wing tip. That corresponds to inserting even more tapper to the already initially tapered geometry. From an aerodynamic perspective, that was expected since introduction of taper ratio leads to a lift distribution closest to the elliptical, therefore reducing the wing drag. Also as the span is fixed, reducing the wing chord, reduces the overall wing area, which increases the aspect ratio of the wing. This set of results shows that the optimizer tried to reduce drag as much as possible. The difference between the initial and the optimized aerodynamic characteristics proves again that the real L-23 wing results from a design process that has taken other disciplinary constraints into account. For a better visualization of the aerodynamic results obtained, Fig. 9 shows the lift and Cp distribution over the wing surface and some sectional data of the optimized L-23 wing.

Comparing the optimization results to the analysis results, it is notable the difference in the lift distributions and Cp values for both cases. The lift distribution evidents the high taper ratio and very small chord at the tip. In sum, the presented results show that, to reduce the drag while fulfilling the C_L constraint, the optimizer had to make changes to the geometry of the wing that had repercussions in its aerodynamic performance. Yet, the optimization was performed successfully, since drag was reduced to the minimum possible when the wing was generating the requested lift, as shown in Fig. 8.

5.3. Structures

Similar to the aerodynamic analysis, there were no imposing requirements for the structural simulations performed. Thus, the conditions chosen are merely academic. The exercise performed consisted in the study of the stresses and deformations of the wing-box structures of the case study, when subjected to a single vertical wing tip nodal load of 500 N. The mechanical properties used for all the wing structures were based on Aluminum 7075, a reference in the aeronautic industry, whose mechanical properties are listed in Table 4.

Table 4: Mechanical properties of Aluminum 7075.

Properties		
Density	2810	Kg/m^3
Young's Modulus	71.7	GPa
Poisson's Ratio	0.33	
Correlation Factor	0.8333	
Yield Strength	434	MPa

The finite-elements used for the structural mesh are based on mixed interpolation of tensorial components approach (MITC) shell elements (Chapelle et al., 2003) and the internal structural layouts of the case study was defined in Sub-section 5.1.

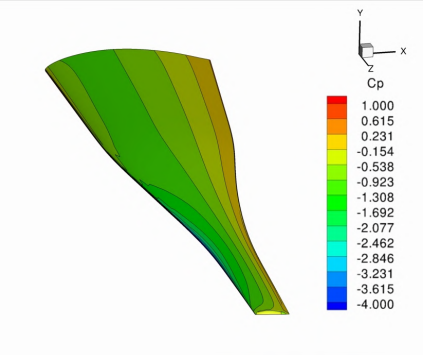

(a) Results for Cp distribution over the wing.

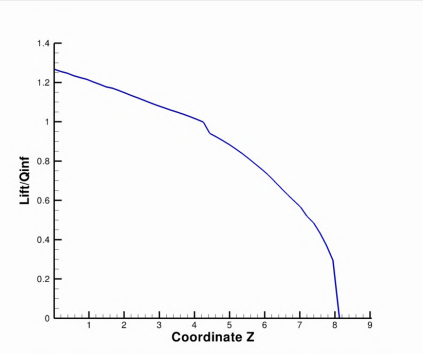

(b) Results for lift distribution over the wing.

Figure 9: Aerodynamic optimization results for the L-23 sailplane wing.

5.3.1 Mesh Convergence Study

To determine how many elements are needed to have a reliable structural mesh discretization a convergence study was performed. The layout chosen for this study was an academic semi-tapered wing. Using the stated exercise, the result studied was the vertical displacement. This was computed for a set of structural meshes, ranging from 6,000 to 22,000 elements. Figure 10 shows the results of the convergence study. To assess the accuracy, the relative

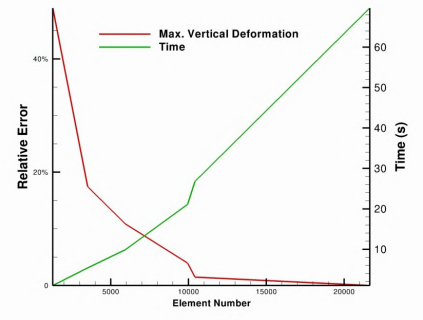

Figure 10: Results for the convergence study between accuracy and element number with *TACS*.

error was used. As the real value of the deformation

was unknown, a reference value given by a mesh refined with 22,000 elements was used. A convergence in the value for the maximum vertical deformation in the structure was verified as the number of elements was increased. Also the time required to perform the structural analysis was measured.

As observable from Fig. 10, the time grows almost linearly with the number of elements used. From the results seen, a total number of elements above 7,500 was considered to give the best relation between accuracy error (approximately 10%) and time to perform the analysis (approximately 13 seconds). This value was used as reference.

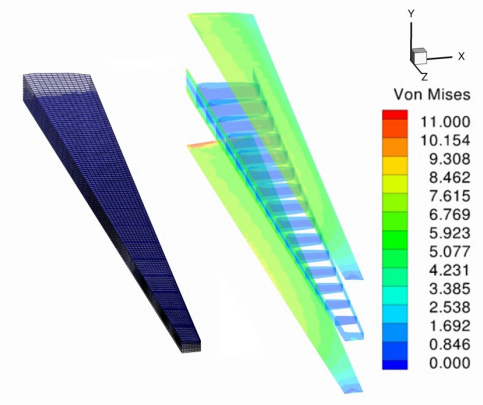

Figure 11: Structural analysis results for the case study.

5.3.2 Structural Analysis

Using the methodology previously described, the structural analysis of the case study was performed.

The deformation results show that the L-23 wing-box has higher stiffness. That was already expected since the structure layout is based on the real L-23 wing-box. Despite the span of the L-23 wing-box is greater than most sailplane aircrafts, it was shown very little deformation as Fig.11 proves. This fact is probably due to the high number of ribs, which enforce the overall structure resistance to bending. Again the L-23 wing shows aspects that justify why the L-23 sailplane is so highly considered for its robustness.

The other results studied were the Von Mises stresses. These give information about how much effort are the components sustaining. The results show important differences between the structural components of the wing-box. As Fig.11 shows, the values of the Von Mises stresses are very small. The maximum values, however, are verified in the lower skin panels at the wing-box root. So, sweep, twist and dihedral angles applied to the wing-box increase the effort made in the bottom skin panels near the root. The higher height of the L-23 wing-box also allows the observation of zones that are sustaining higher stresses within the ribs. From a structural perspective, the L-23 case study shows good results, thus, a wing-box structure with higher height and higher number of ribs presents a better starting point for an MDO of a sailplane wing. In summary, the structures module provided consistent results for the exercised structural analysis. These highlighted the good starting structural design point, that the L-23 wing case is. Although simple, these observations are important in the preliminary design stage, as they can allow the early choice of the better overall structure layout for the main components of the sailplane wing.

5.4. Aero-Structural Optimization

The last exercise performed in the scope of this thesis was an aero-structural optimization. This was also its main objective. The conditions used to simulate the initial flight condition was the same used for the aerodynamic analysis of Sub-section 5.2.2. As for the structural model, the layout and specifications used were already presented in Section 5.1. The methodology was also discussed in Chapter 3.

In addition to the maximization of the L/D ratio, the weight minimization is one of the main objectives in sailplane performance. The weight reduction can maximize the flight endurance. So, the established optimization problem, used to perform the MDO on the case studies, was a drag minimization with a weight constraint, enforcing the weight reduction. As this was an academic study, the requirements for the optimization study were not imposed, so two types of constraints were set. An aerodynamic constraint set to the L/W ratio and a set of structural constraints for the maximum Von Mises stresses. The aerodynamic constraint implied that the lift generated by the wing had to be equal to the sailplane weight. This was not fixed, since reducing the weight of the wing structure was one of the objectives. So a percentage of the initial weight of the sailplane was fixed, allowing the remaining percentage to change according to the wing structures weight. The Von Mises stress constraints were done indirectly through KS function constraints. KS functions are used to aggregate all stresses into a single constraint, for the skin, spar and rib group elements. These were set to the range of 0.3 to 2, which can be interpreted as the minimum safety before failure. So the variation of the structural weight was possible due to the variations on the component thicknesses, (structural) variables in the optimization problem and the variation of lift was possible due to variation of the aerodynamic parameters: angle of attack, twist and scale.

So, the MDO tool established in this thesis was used to perform an aero-structural optimization on the L-23 sailplane wing.

To summarize the results of the aero-structural optimization, a comparison of the initial and optimized design variables and constraints for the case study is given in Table 5. As the number of thickness variables was too long, a median was made for each group of components.

The results of the aero-structural optimization show that its objective was achieved, which was the drag minimization subjected to aerodynamic and structural constraints, enforcing the weight reduction of the structure. Looking to the optimization constraints, all of them have been fulfilled, so a feasible design was generated in the optimization. The aerodynamic parameters show some important aspects of the optimization. The most notorious is the optimized angle of attack, that is lower than the initial. This shows that the optimizer had to decrease the angle of attack to decrease the lift generated. Thus, the initial drag decrease in the starting iterations of the optimization process visible in Fig. 14. The scale of the sections along the span was decreased, introducing a higher taper ratio to the wing. Yet, the scale values were not lowered to the minimum allowed, as was seen in the aerodynamic optimization. This should be expected since that would probably decrease the drag of the wing. However, as the objective was weight reduction, some trade-offs had to be made between the aerodynamic and structural performance. This fact explains the fluctuations in the drag values during the convergence history. Also, decreasing the chord of the wing sections to lower values, would have implications in the structural stiffness of its wing box and, therefore, in the values of the KS constraints. The structural parameters are consistent with the constraint values. The median thickness of the top skin, bottom skin and spar groups were lowered to the minimum possible, therefore reducing the stresses sustained by these components and the value of their KS functions (lowering the associated safety factor). The optimizer chosen to lower these thicknesses so that the lift, generated by the wing surface, could balance the weight of the aircraft. However, the median rib thickness was increased. This explains why the KS function value of the rib group is at the higher bound and why the weight has been optimized to the higher bound value. This may indicate that the optimizer could not lower this value due to the structural constraints. For example, reducing the rib thickness could increase the stresses that had to be sustained by other structural components, which, for instance, would decrease the value of their KS functions to a point where they would not be within the constraint bounds. So this highlights a trade-off made by the optimizer between lowering the structural weight and fulfilling the structural constraints in the presented case study. Figures 12 and 13 shows the results of the aero-structural optimization of the case study. Looking to Fig. 13, one can see the higher deformation of the wing-box when compared to the simple structural analysis exercise. Also the Von Mises stresses comproved that a higher effort is being made by the structural components, the lower skin panels at the wing-box root showing the higher stresses. These results are consistent with the minimum KS function values, which corresponds to the top and bottom skin groups. The Cp and lift distribution over the wing comproved the lower angle of attack in the root sections and the higher angle of attack in the tip sections (due to the local twist applied). Ultimately, the optimization problem was successfully accomplished, as the objective of reducing the weight and drag of the sailplane were achieved while fulfilling the structural and aerodynamic constraints.

Differences from the simple disciplinary optimizations were evident, proving that some trade-offs had to be made between the structural performance and the aerodynamic performance.

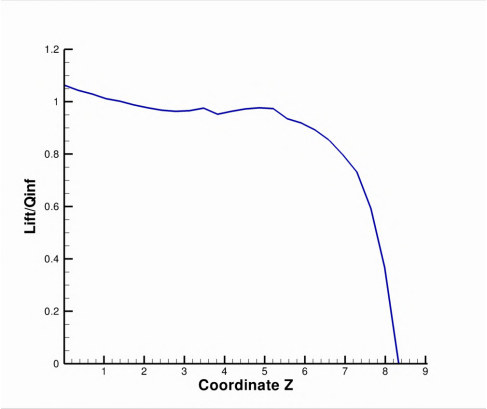

(a) Results for lift distribution over the wing.

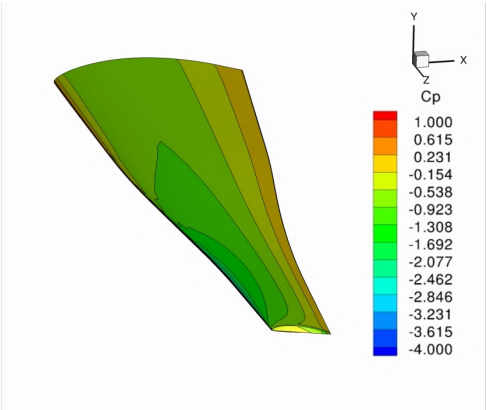

(b) Results for Cp distribution over the wing.

Figure 12: Aero-structural optimization aerodynamic results for the case study.

Table 5: Aero-structural optimization parameters for the L-23 wing.

Parameter	Initial Value	Optimized Value	Lower Bound	Upper Bound	
Total Mass	530	525	0	525	Kg
Vertical resultant force	-	0	0	0	N
KS top skin group	-	0.340	0	2	
KS bottom skin group	-	0.358	0	2	
KS spar group	-	0.353	0	2	
KS rib group	-	2	0	2	
Angle of Attack	3	1.24	-4	7	°
Twist (Four Sections)	0	5	-10	10	°
Chord Scale (Four Sections)	1	0.768	0.5	2	
Median Top Skin Thickness	5	1.5	1.5	10	mm
Median Bottom Skin Thickness	5	1.5	1.5	10	mm
Median Spar Thickness	5	5	5	10	mm
Median Rib Thickness	8	10	1.5	10	mm
C_D	0.00774	0.00687			

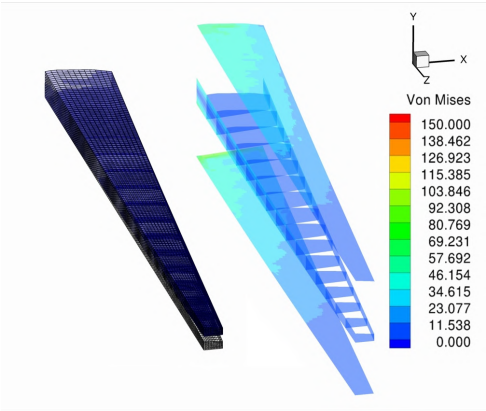

Figure 13: Results for the deformation and Von Mises stresses of the wing structural layout.

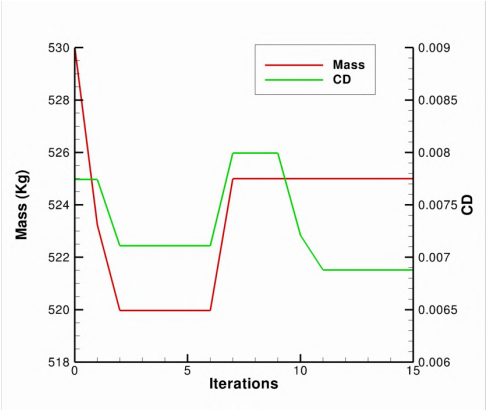

Figure 14: Results for the convergence history for the aero-structural optimization results for the case study. .

6. Conclusions and Future Work

6.1. Achievements and Acquired Knowledge

The motivation for this thesis was to develop knowledge in the field of multi-disciplinary design of aircraft wing configurations. Two core disciplines were considered, aerodynamics and structures, for the objective of this thesis, which was running an aero-structural optimization of sailplane wings. To achieve that objective, an MDO framework was established. This stage was longest step of the realization of this thesis, as the task of coupling and testing the modules often revealed tough. With the MDO tool established, a realistic test was created and used. This test provided deeper knowledge of the behavior of wing geometries and structures in cruise flight condition. Also, worth of mention is the fact that, though, the exercises performed were simple, the formulation of the aero-structural problems was the hardest task. And if this happen with a simple aero-structural MDO exercise, in a real aircraft project, were the number of either disciplines and variables is much higher, the time and effort needed for such task may be unbearable. Maybe this is why MDO is not yet a standard practice in aircraft industry. Still, after the problems have been formulated, the aero-structural optimization run with the established MDO tool performed smoothly.

Finally, from the results obtained with the aero-structural optimization, it was possible to capture the multi-disciplinary trade-offs between what was best in terms of aerodynamics and what was feasible in terms of aero-structural requirements. So, using MDO in preliminary design stage exercises have shown that taking into account more than one discipline can lead to better optimized designs. Having this multi-disciplinary perspective right from the beginning of the aircraft design process can reduce

the feasible design space, allowing resources to be saved from later re-designs.

6.2. Directives for Future Work

Future work in the development of the aerostructural MDO framework established in this thesis is expected. For example, to explore the full capabilities of each of the modules employed, so that more realistic aircraft design problems can be solved. Also, different flight conditions should and can be considered, as its implementation is already possible within the current framework.

Regarding the modules, it would be interesting to improve the geometry module so different aircraft wings could be employed in the MDO framework, as for example wings with lift-enhancement devices. The aerodynamic module *Tripan* could also be so that a method more complex than the panel method could be used for high-fidelity analysis. This would allow the modeling of compressible flows, which would extend the range of flight conditions to be modeled. The structural module *TACS* was the least explored in the exercises performed with the MDO tool. Despite this, future works could use its full potential, for example, in terms of the use of composite materials. Also, an interesting work could consist of a validation of the TACS results with some experimental tests, for example with the Portuguese Air Force sailplanes.

Acknowledgements

The author would like to thank Doctor André Marta for all the support and guidance during the realization of this MSc thesis, and to Graeme Kennedy for the support and availability to help with the MDO toolset usage.

References

Alexandrov, N. and Hussaini, M. (1997). *Multidisciplinary design optimization: state of the art*. Proceedings in Applied Mathematics Series.

Anderson, J. D. (2001). *Fundamentals of Aerodynamics*. McGraw-Hill, third edition.

Balay, S., Buschelman, K., Eijkhout, V., Gropp, W. D., Kaushik, D., Knepley, M. G., McInnes, L. C., Smith, B. F., and Zhang, H. (2004). PETSc users manual. Technical report, Argonne National Laboratory.

Brown, S. (1997). Displacement extrapolation for CFD+CSM aeroelastic analysis. *AIAA Paper 97-1090*.

Chapelle, D., Oliveira, D., and Bucalem, M. (2003). MITC elements for a classical shell model. *Comput. & Structures*.

Dennis, J. and Lewis, R. (1994). Problem formulations and other optimization issues in multidisciplinary optimization. 94-2196.

Gill, P. E. (2008). *User's Guide for SNOPT Version 7: Software for Large-Scale Nonlinear Programming*. Department of Mathematics of University of California.

Hicken, J. and Zingg, D. (2010). A simplified and flexible variant of GCROT for solving nonsymmetric linear systems. *SIAM Journal on Scientific Computing*, 32(3):1672–1694.

Isaacs, A., Sudhakar, K., and Mujumdar, P. M. (2003). Design and development of MDO framework. In *MSO-DMES 2003 Conference Paper*, 78.

Kennedy, G. J. and Martins, J. R. R. A. (2010). Parallel solution methods for aerostructural analysis and design optimization. *13th AIAA/ISSMO Multidisciplinary Analysis Optimization Conference*.

Kenway, G. K., Kennedy, G. J., and Martins, J. R. R. A. (2010). CAD-free approach to high-fidelity aerostructural optimization. *13th AIAA/ISSMO Multidisciplinary Analysis Optimization Conference*, pages 1–3.

LET Aircraft Industries (2011). *L-23 Super-Blanik Sailplane Maintenance Manual*. Portuguese Air Force.

Liebeck, R. H. (2004). Design of the blended wing body subsonic transport. *Journal of Aircraft*, 41(1):10–25.

Martins, J. R. R. A. (2002). *A coupled-adjoint method for high-fidelity aero-structural optimization*. Ph.d. thesis, S. U.

Martins, J. R. R. A. and Tedford, N. P. (2006). On the common structure of MDO problems: A comparison of architectures. In *11th AIAA/ISSMO Multidisciplinary Analysis and Optimization Conference*, AIAA 2006-7080.

MDO Technical Commite, editor (1991). *Current State of the Art in Multidisciplinary Design Optimization*. AIAA.

Perez, R., Liu, H. H. T., and Behdinan, K. (2004). Evaluation of multidisciplinary optimization approaches for aircraft conceptual design. In *AIAA/ISSMO Multidisciplinary Analysis and Optimization Conference*, Albany, NY.

Perez, R. E., Jansen, P. W., and Martins, J. R. (2011). pyOpt: A Python-based object-oriented framework for nonlinear constrained optimization. *Struct & MDO*.

Saad, Y. and H.Schultz, M. (1986). GMRES: A generalized minimal residual algorithm for solving nonsymmetric linear systems. *SIAM Journal on Scientific Computing*.

Schmitt, V. and Charpin, F. (1979). Pressure distributions on the ONERA-M6-wing at transonic mach numbers. *Experimental Data Base for Computer Program Assessment. AGARD AR 138*.

Sederberg, T. W. and Parry, S. R. (1986). Free-form deformation of solid geometric models. *SIGGRAPH Comput. Graph.*, 20:151–160.

Slater, J. W. (2008). ONERA M6 wing: Study 1. `http://www.grc.nasa.gov/WWW/wind/valid/m6wing/m6wing01/m6wing01.html`. Accessed December 2011.

Smith, S. C. (1996). A computational and experimental study of nonlinear aspects of induced drag. Technical report, National Aeronautics and Space Administration.

Sobieszczanski-Sobieski, J. (1988). Optimization by decomposition: A step from hierarchic to non-hierarchic systems. Technical report, NASA Technical Report CP-3031.

Sobieszczanski-Sobieski, J., Jeremy, S. A., and Robert, R. S. J. (1998). Bi-level integrated system synthesis (BLISS). In *National Aeronautics and Space Administration Technical Manual*, NASA/TM-1998-208715. AIAA.

Weide, B. E. V. D., Kalitzin, G., and Schluter, J. (2005). On large scale turbomachinery computations. *CTR Annual Research*, (1981):139–150. Accessed December 2011.

Wrenn, G. (1989). An indirect method for numerical optimization using the Kreisselmeier-Steinhauser function. Nasa technical report cr-4220, National Aeronautics and Space Administration.

Yi, S. I., Shin, J. K., and Park, G. J. (2007). Comparison of MDO methods with mathematical examples. *Structural and Multidisciplinary Optimization*.